Highly active bimetallic nickel catalysts for alternating copolymerization of carbon dioxide with epoxides

Yu-Chia Su,[a] Chih-Hsiang Tsui,[a] Chen-Yen Tsai,[b] and Bao-Tsan Ko*[a]

[a]*Department of Chemistry, National Chung Hsing University, Taichung 402, Taiwan*

[b]*Department of Chemistry, Chinese Culture University, Taipei 111, Taiwan*

*Corresponding author. E-mail addresses: btko@dragon.nchu.edu.tw (B.-T. Ko); Tel: 886-4-22840411-715; Fax: 886-4-22862547.

Fig. S1 ORTEP drawing of complex **2** with probability ellipsoids drawn at 50% level.

Fig. S2 ORTEP drawing of complex **3** with probability ellipsoids drawn at 50% level.

Fig. S3 ORTEP drawing of complex **4** with probability ellipsoids drawn at 60% level.

Fig. S4 ORTEP drawing of complex **5** with probability ellipsoids drawn at 50% level.

Fig. S5 Plot of M_n (■) and PDI (▲) (determined from GPC analysis) *vs* CHO conversion for the copolymerization of CHO and CO_2 using di-nickel acetate complex **1** as the catalyst ($[CHO]_0/[\mathbf{1}]_0 = 10000$) at 120 °C and 20.7 bar CO_2.

Fig. S6 GPC traces for the afforded PCHC with a bimodal molecular weight distribution catalyzed by di-nickel complex **1** (Table 1, entry 10).

Fig. S7 ^{1}H NMR spectrum of the purified PCHC produced at 1 atm of CO_2 pressure by using di-nickel acetate complex **1** (Table 2, entry 1) in $CDCl_3$. Peak at δ 4.65 ppm is assigned to the methine protons in PCHC, and no significant signals at 3.2-3.5 ppm confirms >99% carbonate linkages in PCHC.

Fig. S8 Plot of M_n (■) and PDI (▲) (determined from GPC analysis) *vs* CHO conversion for the copolymerization of CHO and CO_2 using di-Ni complex **1** as the catalyst ($[CHO]_0/[\mathbf{1}]_0 = 1600$) at 80 °C and 1 atm of CO_2 pressure.

Fig. S9 ^{1}H NMR spectrum of the purified PVCHC produced by using di-nickel acetate complex **1** (Table 3, entry 2) in $CDCl_3$. No significant signal at 3.2-3.5 ppm confirm >99% carbonate linkages in PVCHC.

Fig. S10 ^{1}H NMR spectrum of the purified PCPC afforded by using di-nickel acetate complex **1** (Table 3, entry 5) in $CDCl_3$. Peak at δ = 4.9 ppm is assigned to the methine protons in PCPC, and no obvious signal at 3.6–4.0 ppm confirms >99% carbonate linkages in PCPC.

Fig. S11 Plot of M_n (■) and PDI (▲) (determined from GPC analysis) *vs* CPO conversion for the copolymerization of cyclopentene oxide and CO_2 using di-nickel acetate complex **1** as the catalyst ($[CHO]_0/[\mathbf{1}]_0$ = 1600) at 120 ^{o}C and 20.7 bar CO_2.

Fig. S12 The MALDI-TOF spectrum of the obtained PCHC polyol catalyzed by di-Ni complex **1** with the addition of water as a chain transfer agent (Table 3, entry 8).

Fig. S13 The MALDI-TOF spectrum of the obtained PCHC polyol catalyzed by di-Ni complex **1** (Table 3, entry 9).

Fig. S14 The MALDI-TOF spectrum of the obtained PVCHC polyol catalyzed by di-Ni complex **1** (Table 3, entry 10).

Fig. S15 GPC traces for PCHC polyol produced by using di-nickel acetate complex **1** (Table 3, entry 9).

Fig. S16 GPC traces for PVCHC polyol produced by using di-nickel acetate complex **1** (Table 3, entry 10).

Fig. S17 GPC traces for PCPC polyol produced by using di-nickel acetate complex **1** (Table 3, entry 11).

Table S1 Selected bond lengths and angles of nickel complexes **1-5** and **A**[46]

Table S2 Temperature effects of CO_2-CHO copolymerization catalyzed by using di-Ni complex **1**

Table S3 Kinetic studies of CO_2-CHO copolymerization catalyzed by using di-Ni complex **1** at various temperatures (100, 110, 120, 125, 130, 135 ^oC)[a]

Table S4 Kinetic parameters for CO_2-CHO copolymerization catalyzed by using di-Ni complex **1**

Table S5 Crystallographic data of complexes **1-5**

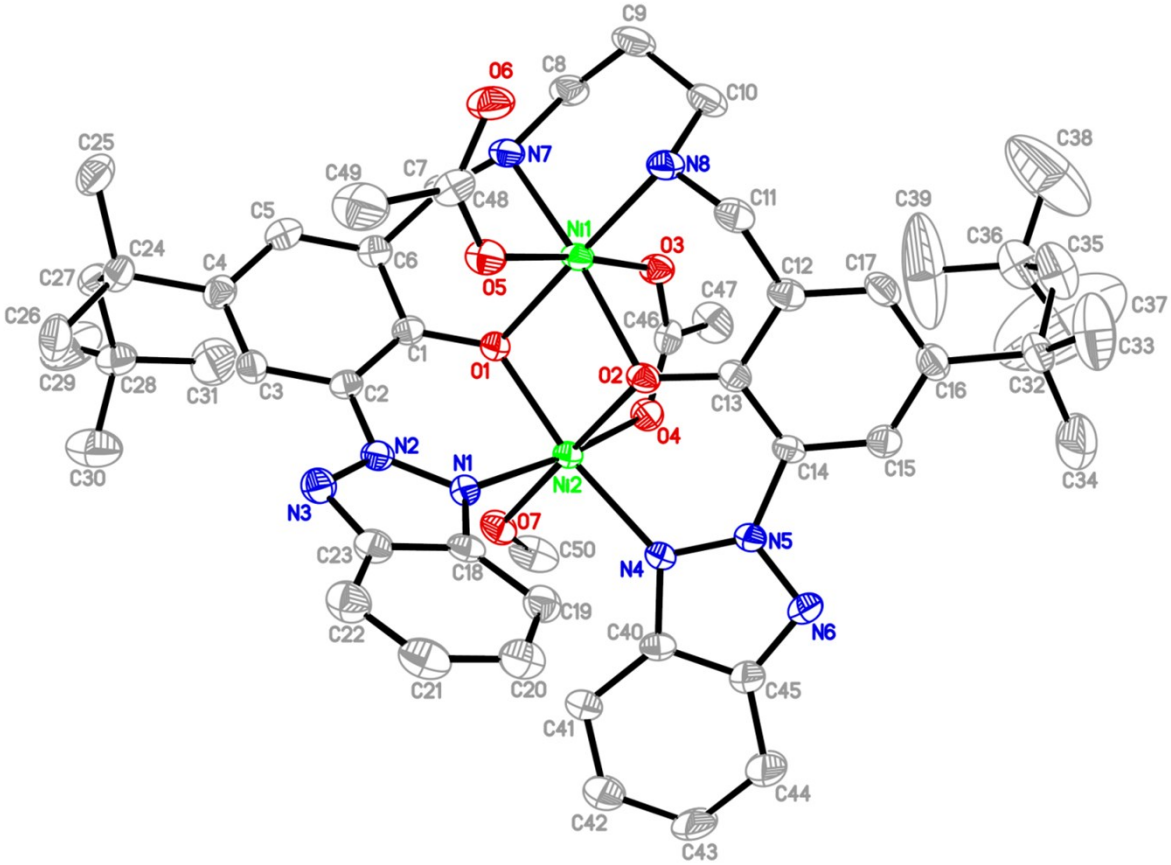

Fig. S1 ORTEP drawing of complex **2** with probability ellipsoids drawn at 50% level. Hydrogen atoms are omitted for clarity. Selected bond lengths/Å and angles/deg: Ni(1)-O(1) 2.008(3), Ni(1)-O(2) 2.128(3), Ni(1)-O(3) 2.054(3), Ni(1)-O(5) 2.067(3), Ni(1)-N(7) 2.106(4), Ni(1)-N(8) 2.030(4), Ni(2)-O(1) 1.970(3), Ni(2)-O(2) 2.047(3), Ni(2)-O(4) 2.037(3), Ni(2)-O(7) 2.090(3), Ni(2)-N(1) 2.113(3), Ni(2)-N(4) 2.040(3), O(1)-Ni(1)-N(8) 178.39(13), O(1)-Ni(1)-O(3) 86.99(11), N(8)-Ni(1)-O(3) 93.55(13), O(1)-Ni(1)-O(5) 87.66(12), N(8)-Ni(1)-O(5) 91.73(14), O(3)-Ni(1)-O(5) 174.17(12), O(1)-Ni(1)-N(7) 88.78(12), N(8)-Ni(1)-N(7) 92.74(14), O(3)-Ni(1)-N(7) 89.15(12), O(5)-Ni(1)-N(7) 93.05(13), O(1)-Ni(1)-O(2) 83.99(11), N(8)-Ni(1)-O(2) 94.51(13), O(3)-Ni(1)-O(2) 88.19(11), O(5)-Ni(1)-O(2) 88.94(11), N(7)-Ni(1)-O(2) 172.42(12), O(1)-Ni(2)-O(4) 88.05(11), O(1)-Ni(2)-N(4) 171.49(12), O(4)-Ni(2)-N(4) 86.91(13), O(1)-Ni(2)-O(2) 87.12(11), O(4)-Ni(2)-O(2) 90.71(11), N(4)-Ni(2)-O(2) 86.10(12), O(1)-Ni(2)-O(7) 93.02(12), O(4)-Ni(2)-O(7) 87.48(13), N(4)-Ni(2)-O(7) 93.60(13), O(2)-Ni(2)-O(7) 178.17(12), O(1)-Ni(2)-N(1) 85.23(12), O(4)-Ni(2)-N(1) 172.11(12), N(4)-Ni(2)-N(1) 100.25(13), O(2)-Ni(2)-N(1) 93.07(12), O(7)-Ni(2)-N(1) 88.76(13).

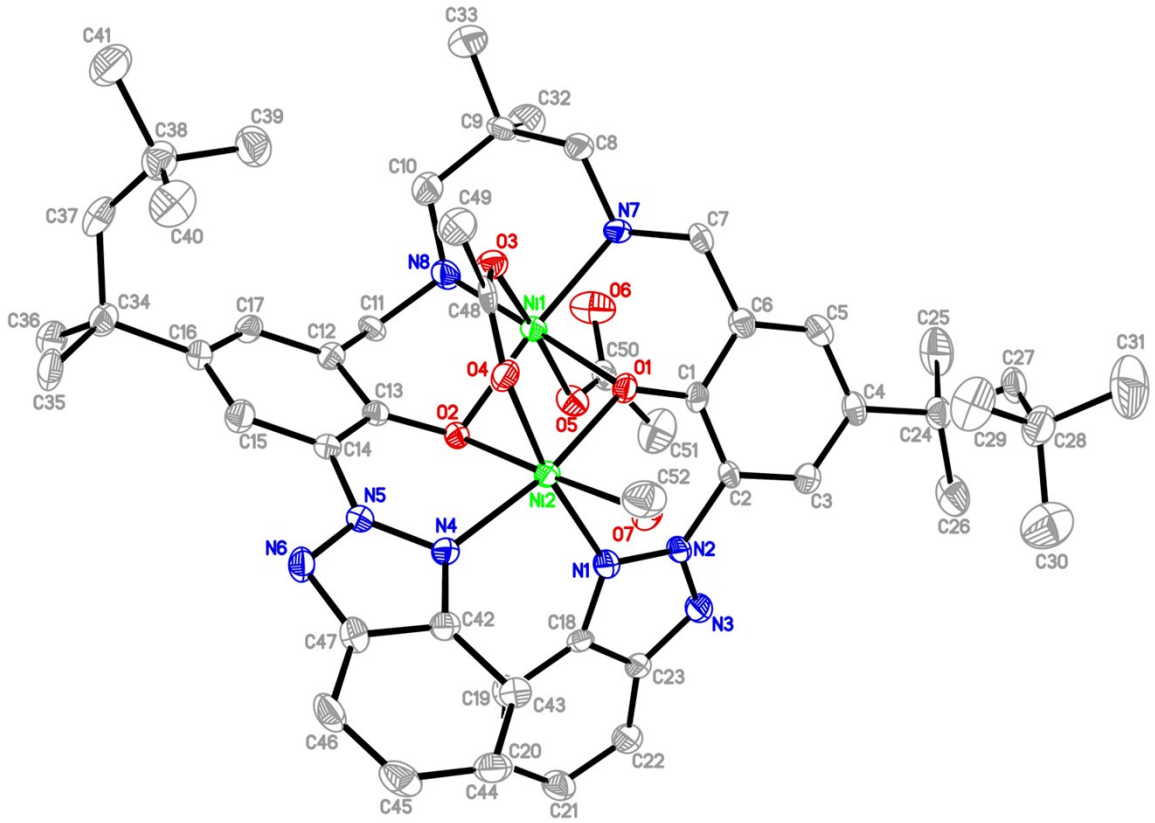

Fig. S2 ORTEP drawing of complex **3** with probability ellipsoids drawn at 50% level. Hydrogen atoms are omitted for clarity. Ni(1)-O(1) 2.009(2), Ni(1)-O(2) 2.130(3), Ni(1)-O(3) 2.069(3), Ni(1)-O(5) 2.083(3), Ni(1)-N(7) 2.096(3), Ni(1)-N(8) 2.029(3), Ni(2)-O(1) 1.974(3), Ni(2)-O(2) 2.066(2), Ni(2)-O(4) 2.045(3), Ni(2)-O(7) 2.116(3), Ni(2)-N(1) 2.124(3), Ni(2)-N(4) 2.045(3), O(1)-Ni(1)-N(8) 178.59(13), O(1)-Ni(1)-O(3) 88.29(10), N(8)-Ni(1)-O(3) 92.90(13), O(1)-Ni(1)-O(5) 87.13(11), N(8)-Ni(1)-O(5) 91.62(13), O(3)-Ni(1)-O(5) 173.29(11), O(1)-Ni(1)-N(7) 89.75(11), N(8)-Ni(1)-N(7) 91.01(13), O(3)-Ni(1)-N(7) 90.30(12), O(5)-Ni(1)-N(7) 94.58(12), O(1)-Ni(1)-O(2) 83.58(10), N(8)-Ni(1)-O(2) 95.69(11), O(3)-Ni(1)-O(2) 88.05(10), O(5)-Ni(1)-O(2) 86.57(10), N(7)-Ni(1)-O(2) 173.17(11), O(1)-Ni(2)-O(4) 88.95(11), O(1)-Ni(2)-N(4) 169.96(12), O(4)-Ni(2)-N(4) 85.66(12), O(1)-Ni(2)-O(2) 86.13(10), O(4)-Ni(2)-O(2) 91.23(10), N(4)-Ni(2)-O(2) 85.53(11), O(1)-Ni(2)-O(7) 92.26(10), O(4)-Ni(2)-O(7) 87.34(10), N(4)-Ni(2)-O(7) 95.93(11), O(2)-Ni(2)-O(7) 177.87(11), O(1)-Ni(2)-N(1) 85.38(11), O(4)-Ni(2)-N(1) 171.61(11), N(4)-Ni(2)-N(1) 100.85(12), O(2)-Ni(2)-N(1) 94.54(11), O(7)-Ni(2)-N(1) 86.72(11).

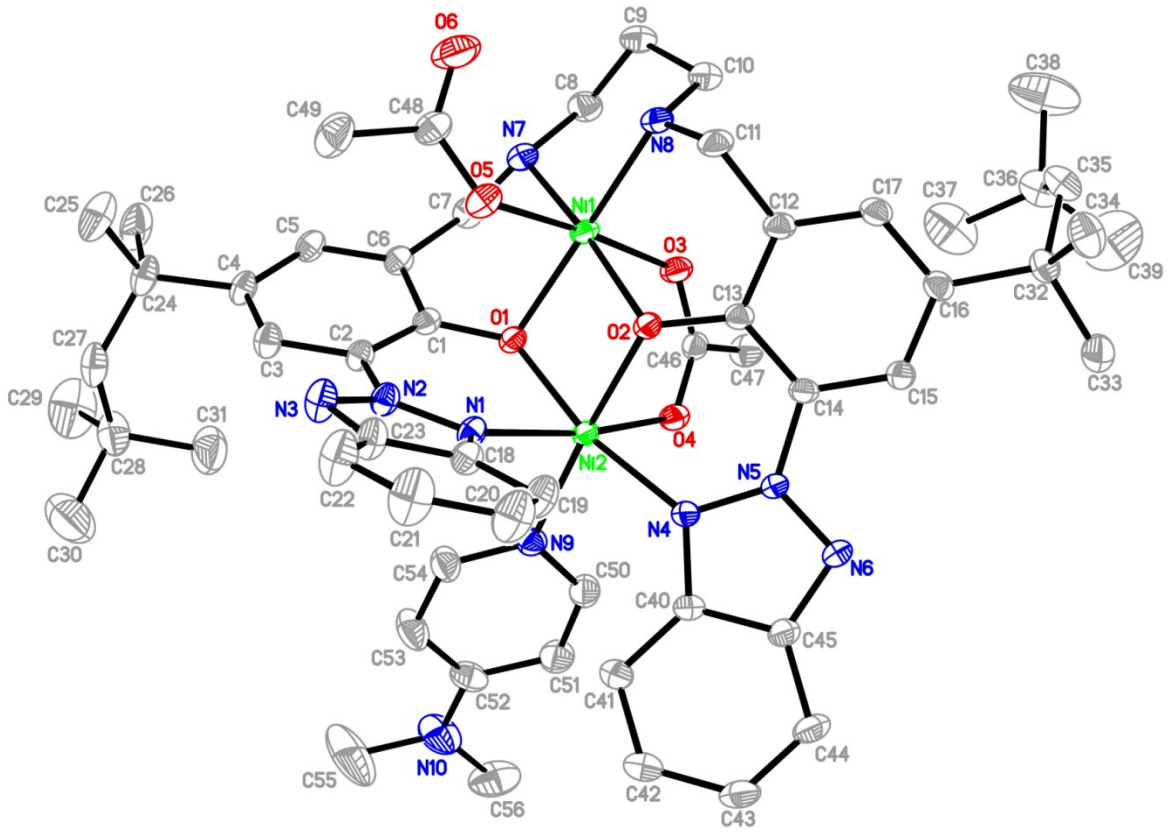

Fig. S3 ORTEP drawing of complex **4** with probability ellipsoids drawn at 60% level. Hydrogen atoms are omitted for clarity. Selected bond lengths/Å and angles/deg: Ni(1)-O(1) 2.0189(10), Ni(1)-O(2) 2.1031(10), Ni(1)-O(3) 2.0666(10), Ni(1)-O(5) 2.0942(11), Ni(1)-N(7) 2.1027(12), Ni(1)-N(8) 2.0281(12), Ni(2)-O(1) 1.9825(10), Ni(2)-O(2) 2.0557(9), Ni(2)-O(4) 2.0835(10), Ni(2)-N(1) 2.1606(11), Ni(2)-N(4) 2.0669(12), Ni(2)-N(9) 2.1084(11), O(1)-Ni(1)-N(8) 177.42(5), O(1)-Ni(1)-O(3) 87.33(4), N(8)-Ni(1)-O(3) 94.86(5), O(1)-Ni(1)-O(5) 89.36(4), N(8)-Ni(1)-O(5) 88.40(5), O(3)-Ni(1)-O(5) 175.78(4), O(1)-Ni(1)-N(7) 89.93(4), N(8)-Ni(1)-N(7) 91.49(5), O(3)-Ni(1)-N(7) 88.47(4), O(5)-Ni(1)-N(7) 94.13(4), O(1)-Ni(1)-O(2) 83.76(4), N(8)-Ni(1)-O(2) 94.94(5), O(3)-Ni(1)-O(2) 87.94(4), O(5)-Ni(1)-O(2) 89.11(4), N(7)-Ni(1)-O(2) 172.88(4), O(1)-Ni(2)-O(2) 85.92(4), O(1)-Ni(2)-N(4) 168.21(4), O(2)-Ni(2)-N(4) 83.91(4), O(1)-Ni(2)-O(4) 86.76(4), O(2)-Ni(2)-O(4) 90.42(4), N(4)-Ni(2)-O(4) 87.36(4), O(1)-Ni(2)-N(9) 96.55(4), O(2)-Ni(2)-N(9) 176.93(4), N(4)-Ni(2)-N(9) 93.43(5), O(4)-Ni(2)-N(9) 87.90(4), O(1)-Ni(2)-N(1) 82.82(4), O(2)-Ni(2)-N(1) 89.28(4), N(4)-Ni(2)-N(1) 102.97(4), O(4)-Ni(2)-N(1) 169.58(4), N(9)-Ni(2)-N(1) 92.83(5).

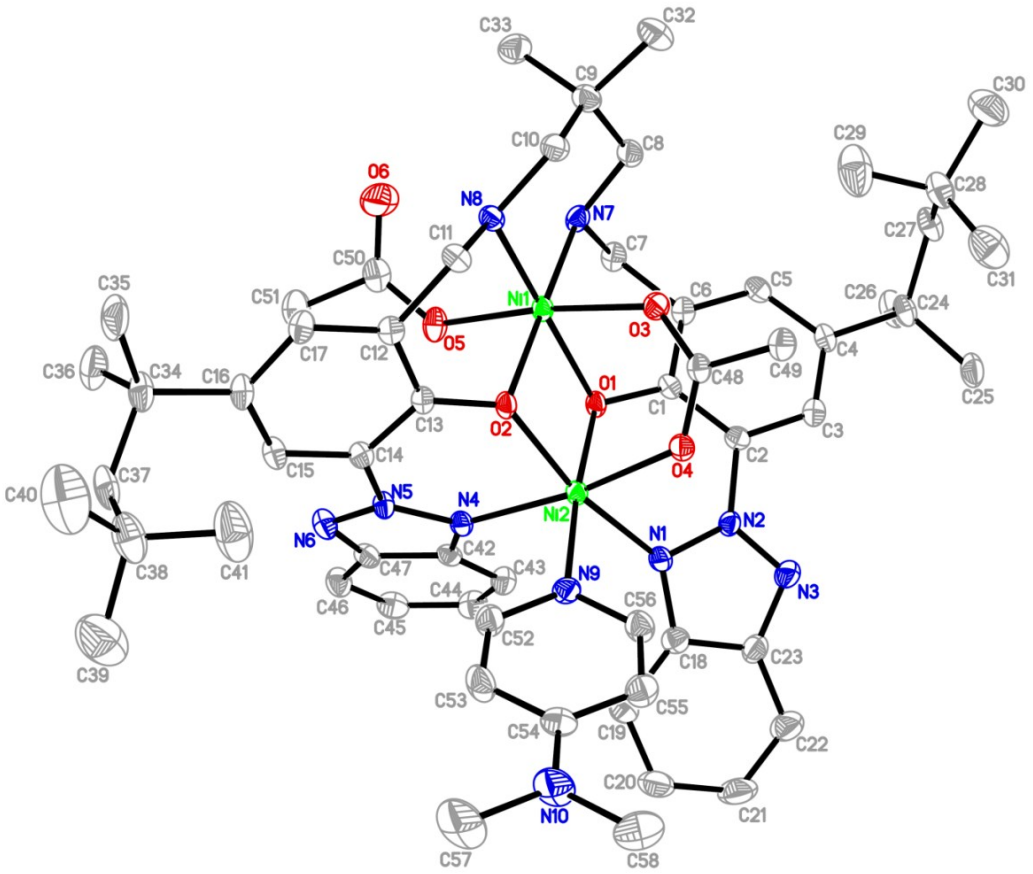

Fig. S4 ORTEP drawing of complex **5** with probability ellipsoids drawn at 50% level. Hydrogen atoms are omitted for clarity. Selected bond lengths/Å and angles/deg: Ni(1)-O(1) 2.111(2), Ni(1)-O(2) 2.019(2), Ni(1)-O(3) 2.072(2), Ni(1)-O(5) 2.081(2), Ni(1)-N(7) 2.029(3), Ni(1)-N(8) 2.089(3), Ni(2)-O(1) 2.063(2), Ni(2)-O(2) 1.983(2), Ni(2)-O(4) 2.068(2), Ni(2)-N(1) 2.064(3), Ni(2)-N(4) 2.143(3), Ni(2)-N(9) 2.096(3), O(2)-Ni(1)-N(7) 178.95(10), O(2)-Ni(1)-O(3) 86.50(9), N(7)-Ni(1)-O(3) 93.73(10), O(2)-Ni(1)-O(5) 89.29(9), N(7)-Ni(1)-O(5) 90.40(10), O(3)-Ni(1)-O(5) 174.07(9), O(2)-Ni(1)-N(8) 90.04(10), N(7)-Ni(1)-N(8) 90.99(11), O(3)-Ni(1)-N(8) 88.65(10), O(5)-Ni(1)-N(8) 95.53(10), O(2)-Ni(1)-O(1) 83.77(9), N(7)-Ni(1)-O(1) 95.23(10), O(3)-Ni(1)-O(1) 86.25(9), O(5)-Ni(1)-O(1) 89.15(9), N(8)-Ni(1)-O(1) 172.20(10), O(2)-Ni(2)-O(1) 85.93(9), O(2)-Ni(2)-N(1) 168.09(10), O(1)-Ni(2)-N(1) 83.82(10), O(2)-Ni(2)-O(4) 87.74(9), O(1)-Ni(2)-O(4) 89.77(9), N(1)-Ni(2)-O(4) 86.18(10), O(2)-Ni(2)-N(9) 96.86(10), O(1)-Ni(2)-N(9) 175.43(10), N(1)-Ni(2)-N(9) 93.00(11), O(4)-Ni(2)-N(9) 86.72(10), O(2)-Ni(2)-N(4) 83.15(10), O(1)-Ni(2)-N(4) 89.97(9), N(1)-Ni(2)-N(4) 102.85(11), O(4)-Ni(2)-N(4) 170.88(10), N(9)-Ni(2)-N(4) 93.96(11).

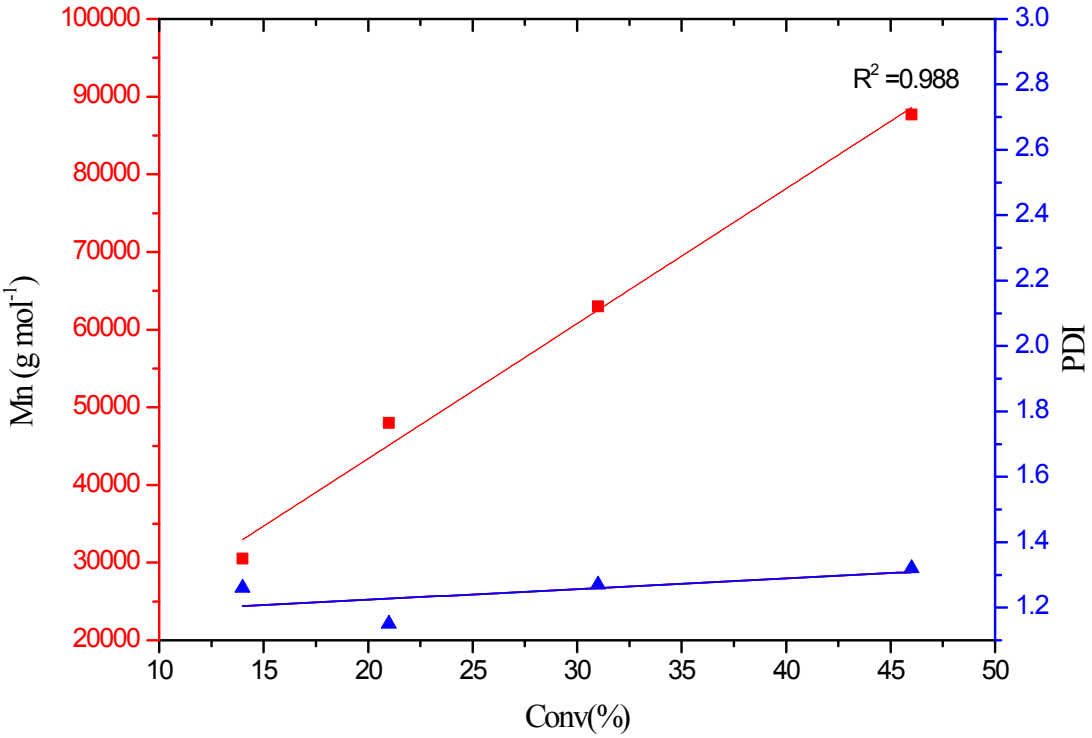

Fig. S5 Plot of M_n (■) and PDI (▲) (determined from GPC analysis) *vs* CHO conversion for the copolymerization of CHO and CO_2 using di-nickel acetate complex **1** as the catalyst ($[CHO]_0/[\mathbf{1}]_0 = 10000$) at 120 °C and 20.7 bar CO_2.

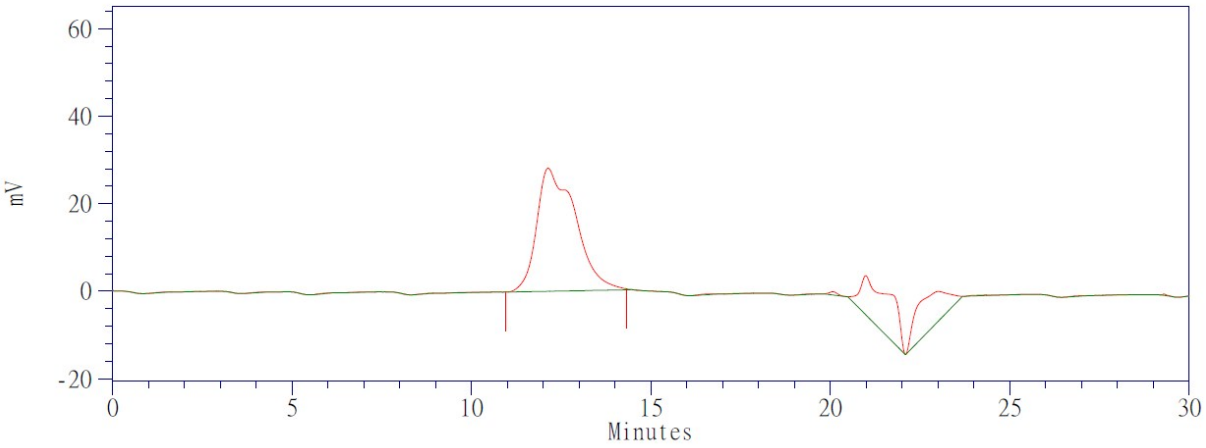

Fig. S6 GPC traces for the afforded PCHC with a bimodal molecular weight distribution catalyzed by di-nickel complex **1** (Table 1, entry 10).

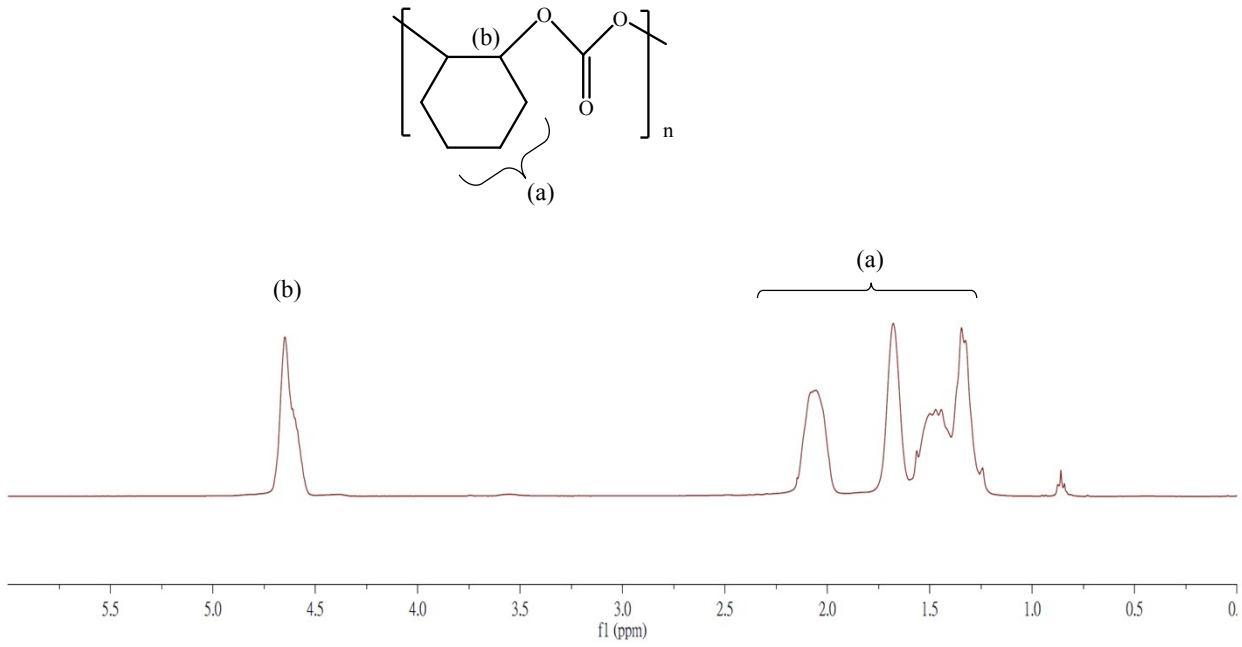

Fig. S7 ^{1}H NMR spectrum of the purified PCHC produced at 1 atm of CO_2 pressure by using di-nickel acetate complex **1** (Table 2, entry 1) in $CDCl_3$. Peak at δ 4.65 ppm is assigned to the methine protons in PCHC, and no significant signals at 3.2-3.5 ppm confirms >99% carbonate linkages in PCHC.

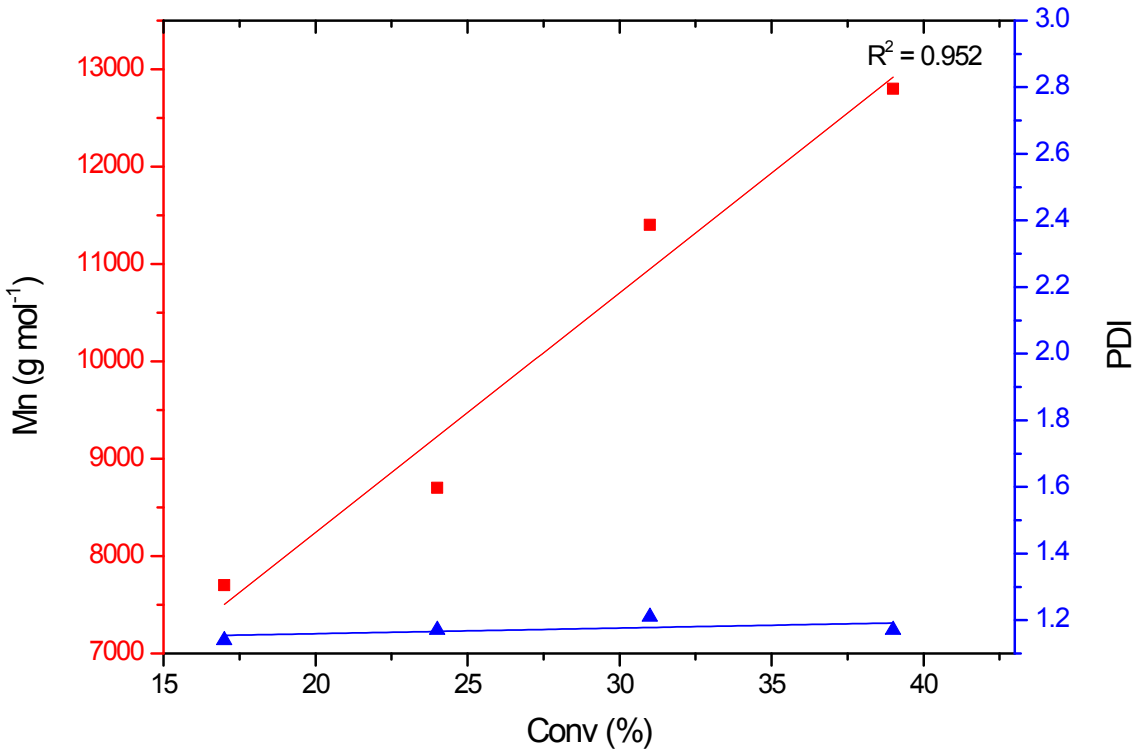

Fig. S8 Plot of M_n (■) and PDI (▲) (determined from GPC analysis) *vs* CHO conversion for the copolymerization of CHO and CO_2 using di-Ni complex **1** as the catalyst ($[CHO]_0/[\mathbf{1}]_0$ = 1600) at 80 °C and 1 atm of CO_2 pressure.

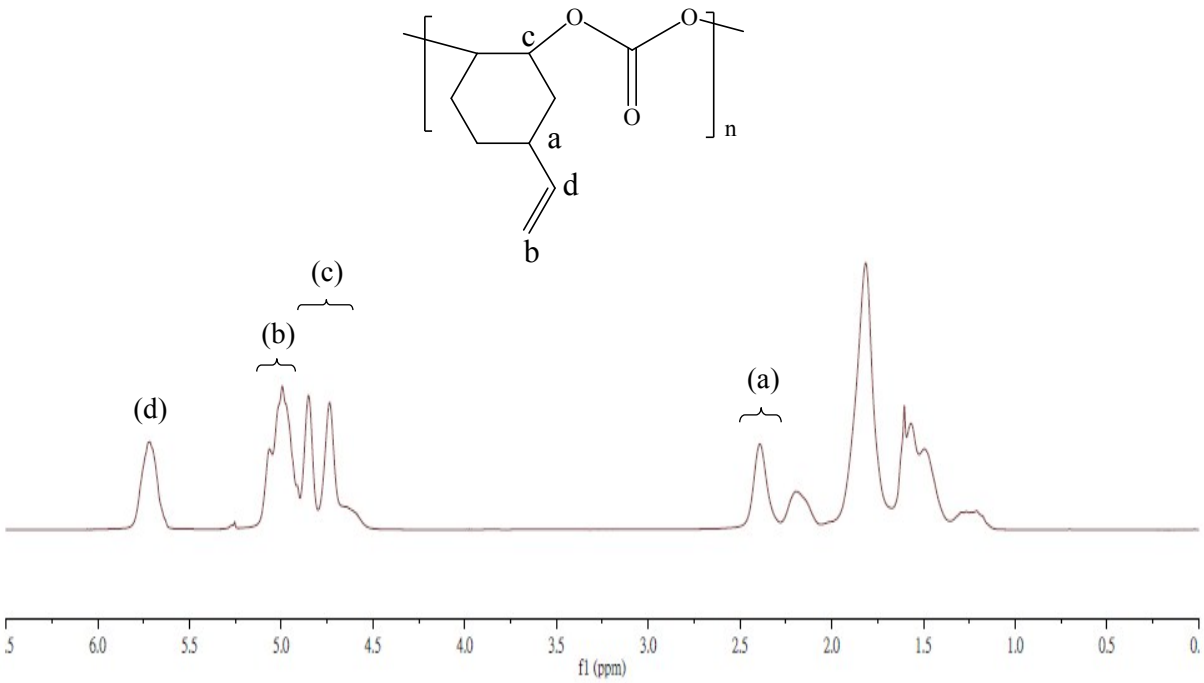

Fig. S9 ^{1}H NMR spectrum of the purified PVCHC produced by using di-nickel acetate complex **1** (Table 3, entry 2) in $CDCl_3$. No significant signal at 3.2-3.5 ppm confirm >99% carbonate linkages in PVCHC.

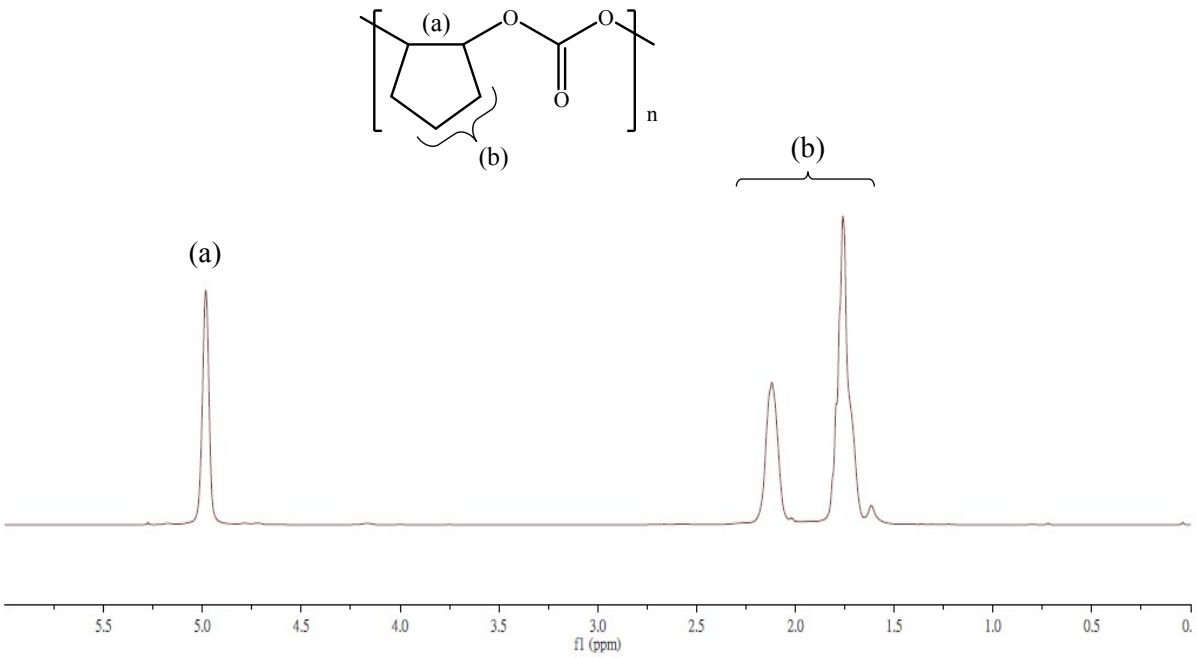

Fig. S10 ^{1}H NMR spectrum of the purified PCPC afforded by using di-nickel acetate complex **1** (Table 3, entry 5) in $CDCl_3$. Peak at δ = 4.9 ppm is assigned to the methine protons in PCPC, and no obvious signal at 3.6–4.0 ppm confirms >99% carbonate linkages in PCPC.

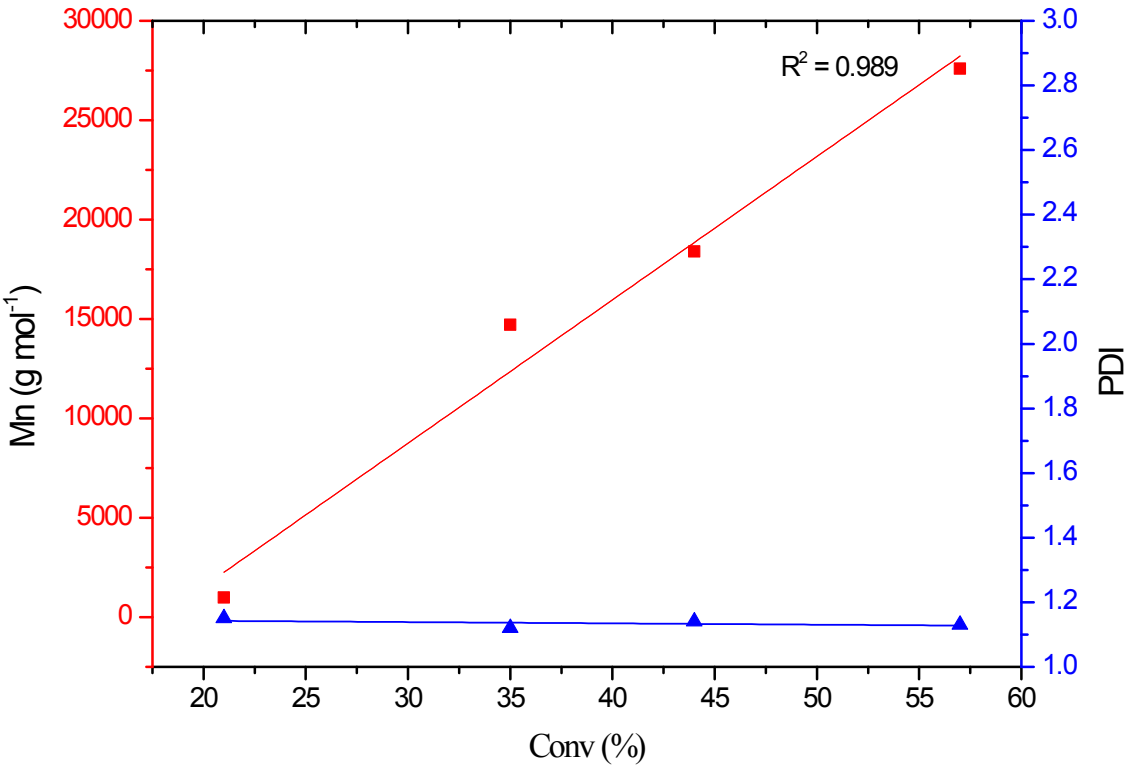

Fig. S11 Plot of M_n (■) and PDI (▲) (determined from GPC analysis) *vs* CPO conversion for the copolymerization of cyclopentene oxide and CO_2 using di-nickel acetate complex **1** as the catalyst ($[CHO]_0/[\mathbf{1}]_0 = 1600$) at 120 °C and 20.7 bar CO_2.

(a)

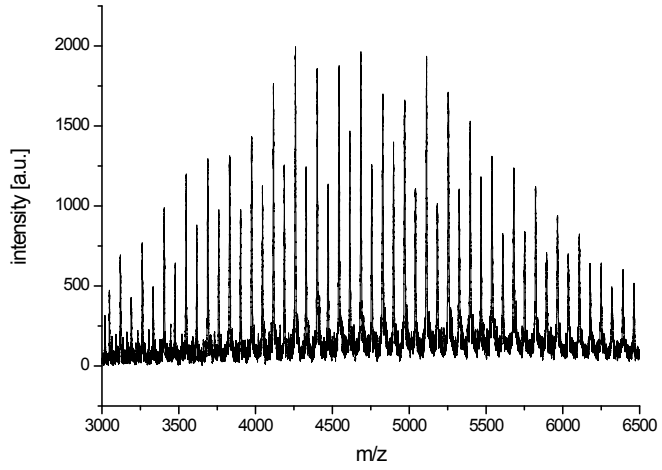

(b)

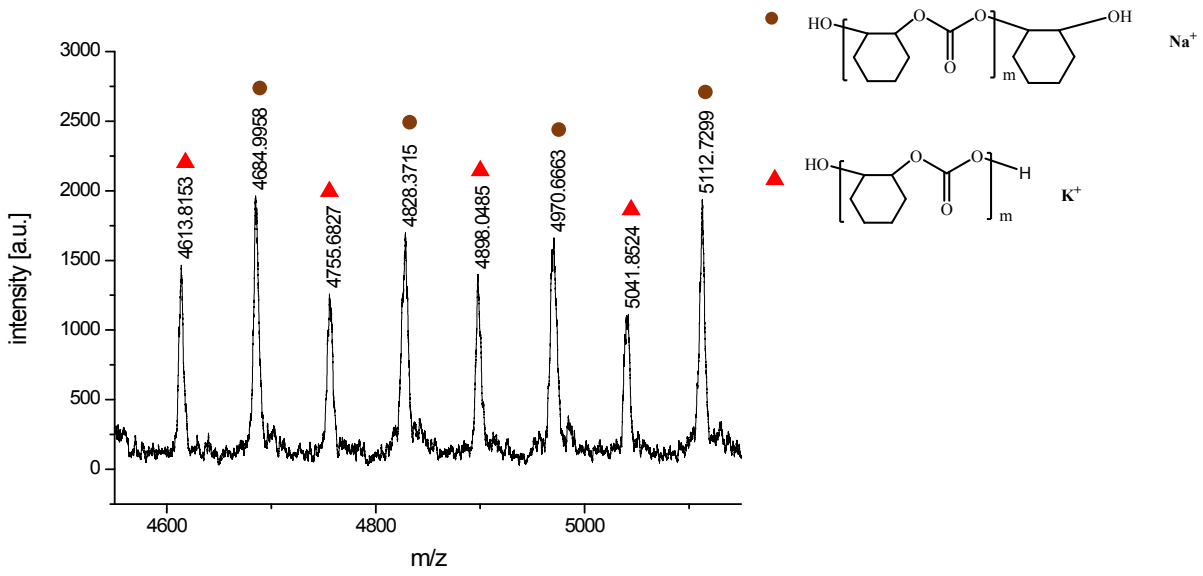

Fig. S12 The MALDI-TOF spectrum of the obtained PCHC polyol catalyzed by di-Ni complex **1** with the addition of water as a chain transfer agent (Table 3, entry 8).

(a)

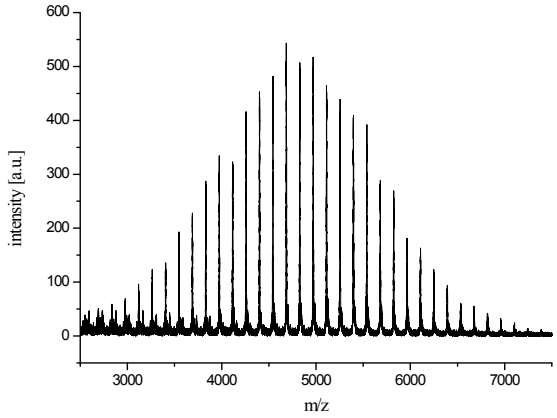

(b)

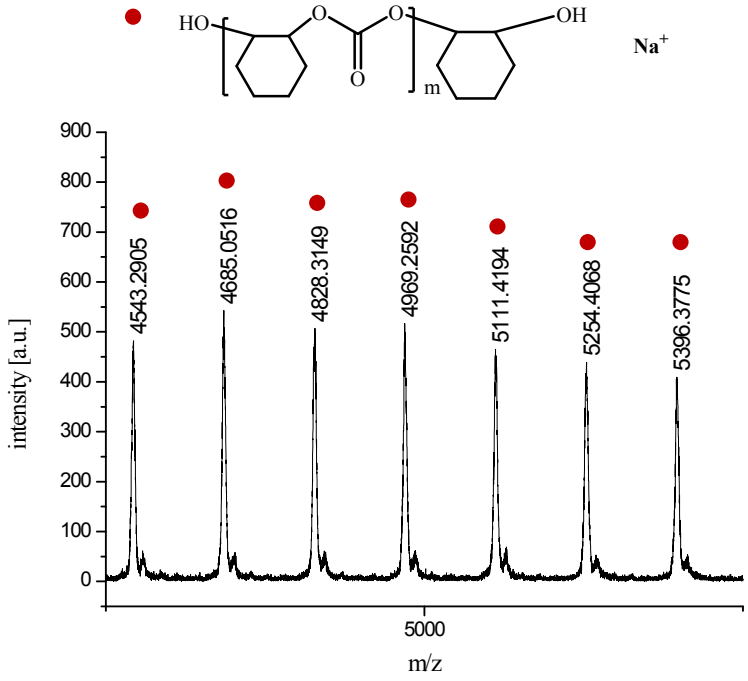

Fig. S13 The MALDI-TOF spectrum of the obtained PCHC polyol catalyzed by di-Ni complex **1** (Table 3, entry 9).

(a)

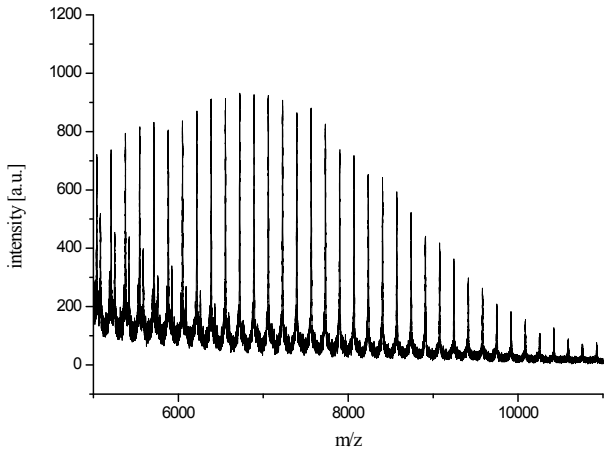

(b)

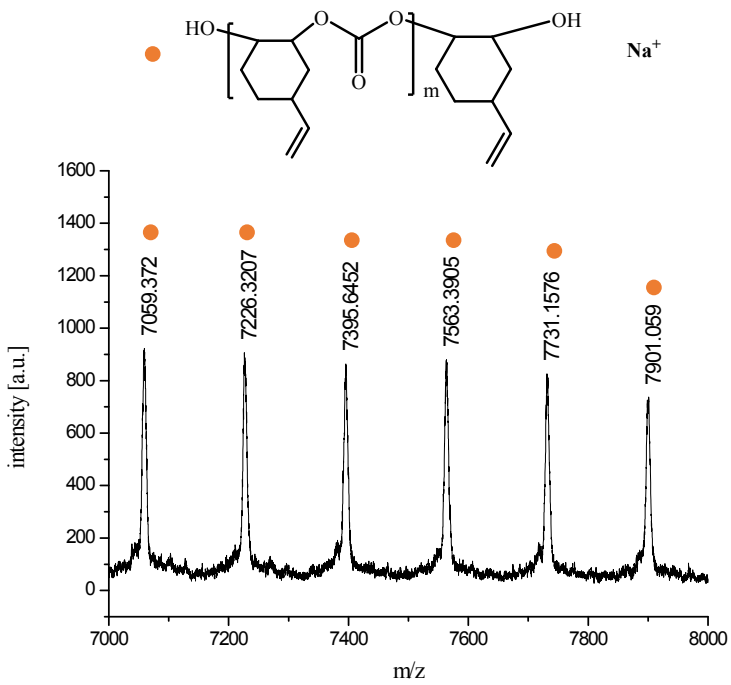

Fig. S14 The MALDI-TOF spectrum of the obtained PVCHC polyol catalyzed by di-Ni complex **1** (Table 3, entry 10).

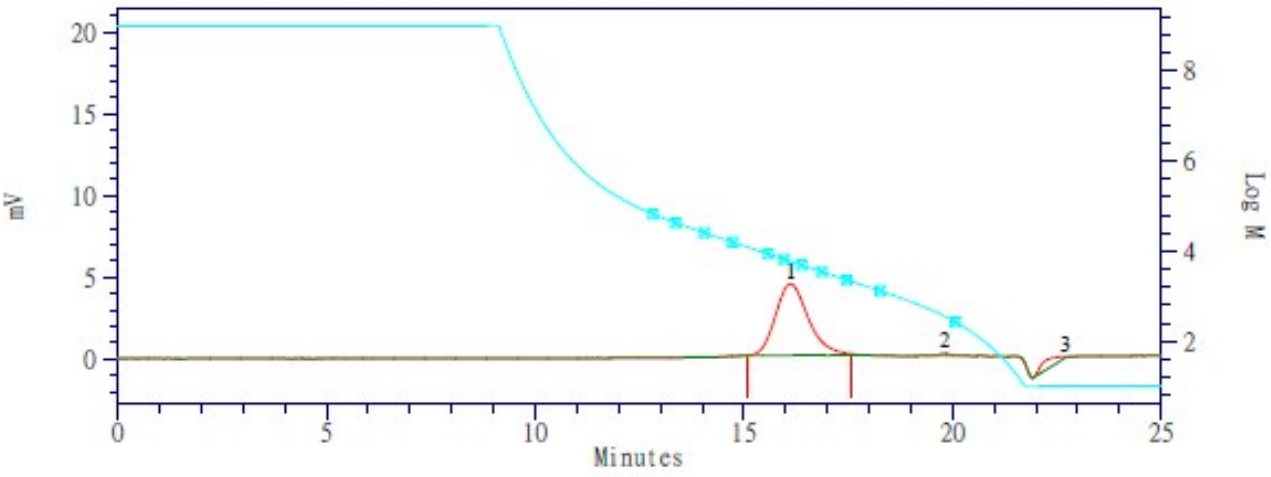

Fig. S15 GPC traces for PCHC polyol produced by using di-nickel acetate complex **1** (Table 3, entry 9).

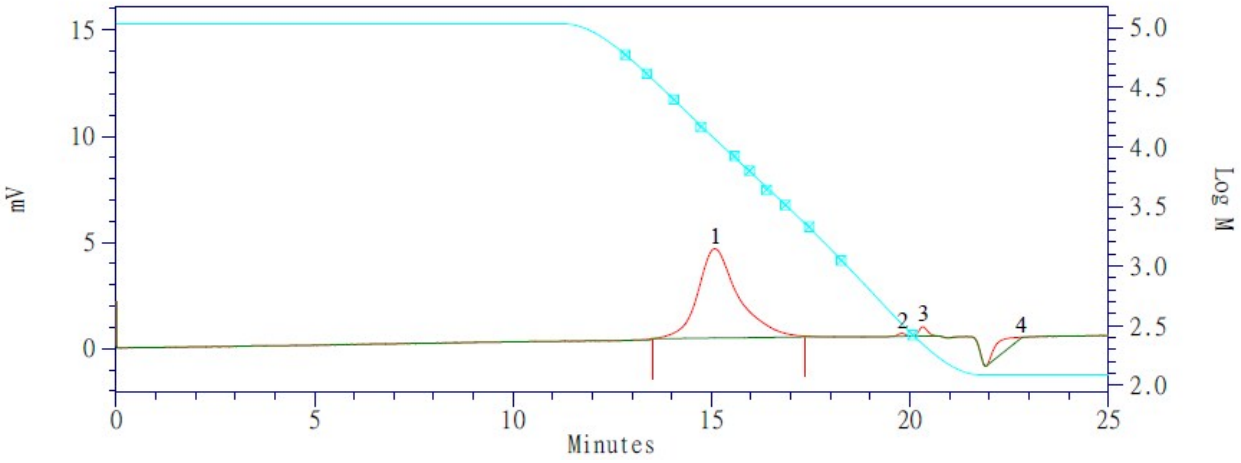

Fig. S16 GPC traces for PVCHC polyol produced by using di-nickel acetate complex **1** (Table 3, entry 10).

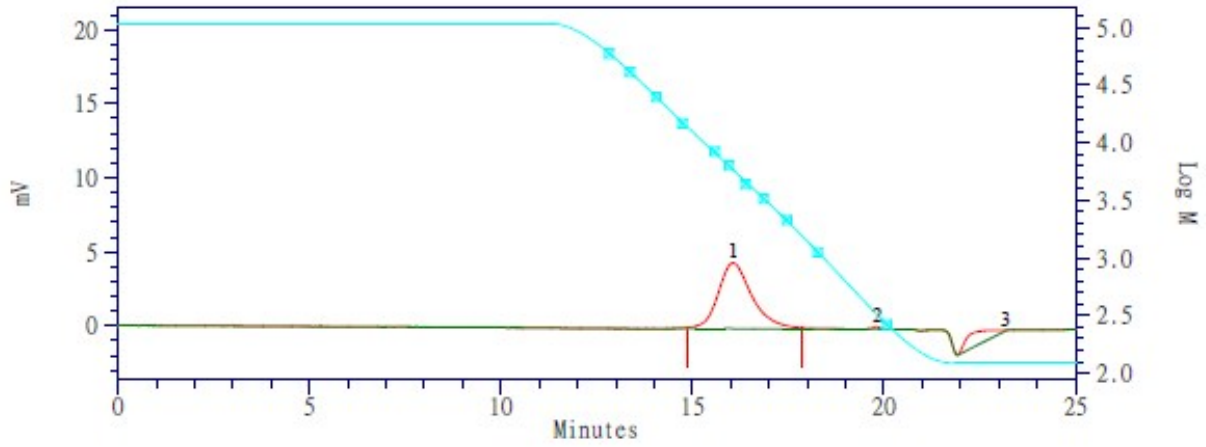

Fig. S17 GPC traces for PCPC polyol produced by using di-nickel acetate complex **1** (Table 3, entry 11).

Table S1 Selected bond lengths and angles of nickel complexes **1-5** and **A**[46]

	1	**2**	**3**	**4**	**5**	**A**
Ni(1)-O(1)	2.028(3)	2.008(3)	2.009(2)	2.0189(10)	2.111(2)	2.0300(17)
Ni(1)-O(2)	2.100(3)	2.128(3)	2.9797(7)	2.1031(10)	2.019(2)	2.0412(17)
Ni(1)-O(3)	2.060(3)	2.054(3)	2.069(3)	2.0666(10)	2.072(2)	2.1142(19)
Ni(1)-O(7)	2.094(3)	-	-	-	-	-
Ni(1)-O(5)	-	2.067(3)	2.083(3)	2.0942(11)	2.081(2)	-
Ni(1)-N(7)	2.126(4)	2.106(4)	2.096(3)	2.1027(12)	2.029(3)	2.074(2)
Ni(1)-N(8)	2.128(4)	2.030(4)	2.029(3)	2.0281(12)	2.089(3)	2.100(2)
Ni(2)-O(1)	1.987(3)	1.970(3)	1.974(3)	1.9825(10)	2.063(2)	2.0606(17)
Ni(2)-O(2)	2.047(3)	2.047(3)	2.066(2)	2.0557(9)	1.983(2)	1.9995(17)
Ni(2)-O(4)	2.106(3)	2.037(3)	2.045(3)	2.0835(10)	2.068(2)	-
Ni(2)-O(5)	2.044(3)	-	-	-	-	2.0283(18)
Ni(2)-N(9)	-	-	-	2.1084(11)	2.096(3)	-
Ni(2)-O(7)	-	2.090(3)	2.116(3)	-	-	2.0731(19)
Ni(2)-N(1)	2.089(4)	2.113(3)	2.124(3)	2.1606(11)	2.064(3)	2.066(2)
Ni(2)-N(4)	2.041(3)	2.040(3)	2.045(3)	2.0669(12)	2.143(3)	2.213(2)
O(1)-Ni(1)-O(2)	82.26(11)	83.99(11)	83.58(10)	83.76(4)	83.77(9)	78.92(7)
O(3)-Ni(1)-O(5)	-	174.17(12)	173.29(11)	175.78(4)	174.07(9)	-
O(3)-Ni(1)-O(7)	174.95(13)	-	-	-	-	-
N(7)-Ni(1)-N(8)	99.22(13)	92.74(14)	91.01(13)	91.49(5)	90.99(11)	86.08(8)
O(1)-Ni(1)-N(8)	169.82(13)	178.39(13)	178.59(13)	177.42(5)	172.20(10)	168.38(8)
O(2)-Ni(1)-N(7)	164.46(12)	172.42(12	173.17(11)	172.88(4)	178.95(10)	105.03(8)
N(1)-Ni(2)-N(4)	102.44(14)	100.25(13)	100.85(12)	102.97(4)	92.37(7)	100.49(8)
O(4)-Ni(2)-O(7)	-	87.48(13)	87.34(10)			-
O(4)-Ni(2)-N(9)	-	-	-	87.90(4)	86.72(10)	-
O(4)-Ni(2)-O(5)	171.14(12)	-	-	-	-	-
O(1)-Ni(2)-O(2)	84.61(11)	87.12(11)	86.13(10)	85.92(4)	85.93(9)	79.17(7)
O(2)-Ni(2)-N(1)	166.66(13)	93.07(12)	94.54(11)	89.28(4)	168.09(10)	163.28(8)
O(1)-Ni(2)-N(4)	169.57(13)	171.49(12)	169.96(12)	168.21(4)	170.88(10)	102.86(7)

Table S2 Temperature effects of CO_2-CHO copolymerization catalyzed by using di-Ni complex **1**

Entry	Temp (°C)	Time /h	% CHO Conv.[a]	% Copolymer[a] (% carbonate)[b]	TON[c]	TOF /h^{-1}[d]	M_n (PDI)[e]
S1	60	4	13	>99(>99)	650	163	17300(1.22)
S2	50	8	12	>99(>99)	600	75	18500(1.22)
S3	25	72	9	>99(>99)	450	6	11100(1.17)
S4[f]	25	72	25	>99(>99)	400	6	12000(1.20)

Copolymerization conditions: 3.125 x 10^{-2} mmol catalyst, $[CHO]_0/[\mathbf{1}]_0 = 5000$, $pCO_2^0 = 20.7$ bar. [a]Based on ^{1}H NMR analysis of the reaction mixture.[43,44] [b]Based on ^{1}H NMR determination of the purified copolymers.[43,44] [c]TON = number of moles of CHO consumed per mole of catalyst. [d]TOF = TON per hour. [e]Determined by GPC in THF, calibrated using polystyrene standards. [f]$[CHO]_0/[\mathbf{1}]_0 = 1600$.

Table S3 Kinetic studies of CO_2-CHO copolymerization catalyzed by using di-Ni complex **1** at various temperatures (100, 110, 120, 125, 130, 135 °C)[a]

Entry	Temp (°C)	Time/min	% CHO Conv.[b]	$\ln([CHO]_0/[CHO]_t)$
S1	100	60	5	0.0513
S2	100	120	16	0.1744
S3	100	180	30	0.3567
S4	100	240	46	0.6162
S5	110	30	22	0.2485
S6	110	60	32	0.3857
S7	110	90	42	0.5447
S8	110	120	50	0.6931
S9	120	20	14	0.1508
S10	120	30	21	0.2357
S11	120	45	31	0.3711
S12	120	60	36	0.4463
S13	125	20	12	0.1278
S14	125	30	23	0.2614
S15	125	45	33	0.4005
S16	125	60	43	0.5621
S17	130	20	14	0.1508
S18	130	30	24	0.2744
S19	130	45	37	0.4620
S20	130	60	49	0.6733
S21	135	20	15	0.1625
S22	135	30	30	0.3567
S23	135	45	44	0.5798
S24	135	60	57	0.8440

Copolymerization conditions: 3.125 x 10^{-2} mmol catalyst, $[CHO]_0/[\mathbf{1}]_0$ = 10000, pCO_2^0 = 20.7 bar. [a]All runs showed excellent copolymerization selectivity (>99% PCHC, >99% carbonate linkages) based on ^{1}H NMR determination. [b]Based on ^{1}H NMR analysis of the reaction mixture.[43,44]

Table S4 Kinetic parameters for CO_2-CHO copolymerization catalyzed by using di-Ni complex **1**

Entry	Temp (^oC)	Observed rate coefficient, k_{obs} (h^{-1})[a]	ln(k_{obs})	Temp (K)	$Temp^{-1}$, 1/T (K^{-1})
S1	100	0.1877	-1.6729	373.15	0.00268
S2	110	0.2986	-1.2087	383.15	0.00261
S3	120	0.4497	-0.7992	393.15	0.00254
S4	125	0.6352	-0.4538	398.15	0.00251
S5	130	0.7783	-0.2506	403.15	0.00248
S6	135	1.0011	0.0011	408.15	0.00245

[a]Calculated from the slope of the fitted regression line of Fig. 4.

Table S5 Crystallographic data of complexes **1-5**

	1·MeOH	**2·MeOH**	**3·3MeOH**	**4·C_6H_{14}·H_2O**	**5·C_6H_{14}·CH_2Cl_2**
formula	$C_{52}H_{76}N_8Ni_2O_8$	$C_{51}H_{72}N_8Ni_2O_8$	$C_{55}H_{84}N_8Ni_2O_{10}$	$C_{62}H_{90}N_{10}Ni_2O_7$	$C_{65}H_{94}Cl_2N_{10}Ni_2O_6$
Formula weight	1058.62	1042.59	1134.72	1204.83	1296.54
Temp (K)	150(2)	150(2)	150(2)	150(2)	150(2)
Crystal system	Monoclinic	Monoclinic	Monoclinic	Triclinic	Triclinic
Space group	*P*2(1)/c	*P*2(1)/c	*P*2(1)/c	*P*-1	*P*-1
a (Å)	16.442(3)	27.590(2)	13.3819(4)	13.7399(12)	13.8204(7)
b (Å)	28.884(5)	11.4039(9)	22.5315(7)	13.7733(13)	14.0460(8)
c (Å)	11.4674(18)	17.0846(14)	19.0121(8)	17.2885(16)	17.8074(10)
α (deg)	90	90	90	81.371(4)	98.3638(19)
β (deg)	108.553(6)	101.680(4)	95.058(3)	73.997(3)	99.7094(18)
γ (deg)	90	90	90	86.306(4)	99.0951(19)
V(Å^3)	5163.0(15)	5264.0(7)	5710.1(3)	3108.4(5)	3311.4(3)
Z	4	4	4	2	2
D_{calc}(Mg/m^3)	1.362	1.316	1.320	1.270	1.289
μ (Mo Kα)(mm^{-1})	0.790	0.774	0.722	0.664	0.706
F(000)	2256	2216	2424	1256	1356
Reflections collected	137484	128026	47943	117356	69634
No. of parameters	644	654	694	722	782
Indep. reflns (R_{int})	9541(0.1015)	10812(0.0956)	12400(0.1059)	32060(0.0231)	13644(0.0714)
$R1[I > 2\sigma(I)]$	0.0755	0.0655	0.0642	0.0516	0.0572
w$R2$ $[I > 2\sigma(I)]$	0.1397	0.1688	0.1224	0.1344	0.1455
Goodness-of-fit on F^2	1.032	1.023	1.023	1.022	1.027